Journal of Thermal Analysis and Calorimetry (2019) 135:3085–3093
https://doi.org/10.1007/s10973-018-7544-9

Flame retardancy and thermal degradation properties of polypropylene/wood flour composite modified with aluminum hypophosphite/melamine cyanurate

Panpan Zhao[1] · Chuigen Guo[1] · Liping Li[1]

Received: 25 March 2018 / Accepted: 9 July 2018 / Published online: 13 July 2018

Abstract
In this study, aluminum hypophosphite (AP) and melamine cyanurate (MCA) were used as flame retardant in polypropylene (PP)/wood flour (WF) composite. The flammability of the PP/WF composites was examined by the limiting oxygen index (LOI), vertical burning test (UL-94) and cone calorimeter test. When the PP/WF composite was loaded with 20% AP/MCA (the mass ratio of AP and MCA was 5: 1), the UL-94 achieved V-0 rating and the LOI was increased to 29.5%. In addition, the flexural strength was increased by about 11.0%. The results of cone calorimeter test revealed that the heat release rate and heat release rate peak of the PP/WF composite with AP/MCA were significantly reduced. The thermal degradation mechanism of PP/WF composites was investigated by thermo-gravimetric analysis, Fourier transform infrared spectrometry, energy-dispersive X-ray spectroscopy and scanning electron microscopy. The results indicate that AP/MCA had the effect of gas-phase and condensed-phase flame retardancy during the combustion and degradation of PP/WF composite. Consequently, a thermal property reinforcing mechanism of the PP/WF composite with AP/MCA was presented.

Keywords Aluminum phosphate · Melamine cyanurate · Wood flour · Flame retardance

Introduction

Nowadays, wood-plastic composites (WPCs) play an increasing role as interior and exterior building materials with an increasing market potential [1, 2]. WPC is a kind of biocomposite that consists of varying contents of wood particles, thermoplastic plastics and additives [3]. WPCs combine the admirable properties of both materials with enhancive long-term performance, cost-effectiveness and three-dimensional moldability. The main applications of WPCs are packaging, logistics, furniture, automotive, landscape, military industry, construction industry and others [4–7].

Due to the high heating value of thermoplastic plastics, WPCs are more sensitive to flame than wood [8]. To extend the field of WPCs application to areas requiring materials with low fire risk, developing flame-retarded WPCs is necessary [9]. Introducing flame retardants (FRs) into materials is the most expeditious method to improve the flame retardancy of materials [10–14]. Halogenated flame retardants have been used for many years due to their effectiveness. However, concerns with respect to smoke toxicity and corrosiveness have enforced industry to seek for a substitute [15]. Halogen-free flame retardants attract great attention owing to environmental protection and availability. Among the halogen-free flame retardants, the intumescent flame retardants (IFRs) have been increasingly applied to flame-retarded WPC. In practice, an IFR additive is a system including an acid source, a blowing agent, and a charring agent or char [16]. Flame-retarding wood or biocomposites have no need of charring agent, because the heteroatoms of cellulose and the aromatic rings of lignin can act as charring agents for residue formation [17].

Among many intumescent flame retardants, a traditional and widely researched IFRs system is based on ammonium polyphosphate (APP). However, higher loading of APP is

✉ Liping Li
lilipingguo@126.com

[1] College of Materials and Energy, South China Agricultural University, Guangzhou 510642, China

always suggested for increasing the flame retardancy, leading to poor mechanical properties because of inferior compatibility in composites [18]. Aluminum hypophosphite (AP) as a novel halogen-free flame retardant is widely used in engineering plastics polyester and received good results [19, 20]. AP has relatively high content of phosphorus that can promote more char produce, acting as an excellent acid source. Melamine cyanurate (MCA), an environment friendly and N-based flame retardant, acts as a blowing agent [21, 22]. Yan et al. [23] prepared flame-retardant polystyrene (PS) using aluminum hypophosphite (AP) and found that AP can release PH_3 which can be oxidized to generate H_3PO_4 catalyzing the formation of char layer. Wu et al. [24] used AHP and MCA to prepare flame-retardant acrylonitrile–butadiene–styrene (ABS). The study showed that AHP and MCA had good synergistic effect when they were used to prepare flame-retardant ABS. However, the flame-retardant properties and mechanism of WPC flame retarded by AP/MCA are seldom reported in the literature.

In this study, the flame-retardant polypropylene/wood flour (PP/WF) composite was prepared by using aluminum hypophosphite (AP) and melamine cyanurate (MCA) via melt blending, and the flame retardancy and mechanical properties of PP/WF composite were investigated. The PP/WF composite loaded with 20% AP/MCA possessed higher flame retardant and flexural strength. During thermal decomposition, more uniform char layer is formed giving rise to higher flame retardation of condensation phase.

Experiment

Materials

Wood flour (WF) was purchased from Harbin Yongxu in China with 80 mesh sieve. Polypropylene (PP) was purchased from Daqing Petrochemical Company in China with the density of 0.89–0.91 g cm^{-3}. Antioxidants 1010 were purchased from Jiangsu Hangguang Company in China. Polypropylene grafted with maleic anhydride (MA-g-PP) was purchased from Hangzhou Haiyi polymer material Ltd. in China. Aluminum hypophosphite (AP) was purchased from Qingdao Fu Muslim Chemical Technology Co. in China. Melamine cyanurate (MCA) was purchased from Shandong Shian Chemical Co. in China.

Sample preparation

The WF was dried at 85 °C for 5–8 h in an electric thermostatic drying oven (DHG-9075A, produced by Shanghai Yiheng Instrument Co., Ltd.) before the experiment. PP, AP and MCA were dried at 60 °C for 4–6 h. The formula of samples is shown in Table 1. Then the dried materials were mixed uniformly in a high-speed grinder (FW-80, produced by Tianjin Teste Instrument Co., Ltd.). The samples were prepared by torque rheometer (RM-200, produced by Harbaugh Electric Manufacturing Co., Ltd.) at 180 °C for 8 min and pressed on a curing machine at 180 °C for 20 s, and then the sheets were formed by high-pressure cooling to test.

Measurements

The limited oxygen index (LOI)

LOI was measured by a JF-3 Oxygen Index Meter (Jiangning Analysis Instrument Company, China) as standard ASTM D-2863. The specimen dimension used was 130 mm × 6.5 mm × 3 mm. Five replicates were tested for each group.

The UL-94 vertical tests

The UL-94 vertical test was measured by a CFZ-3 Vertical Burning Instrument (Jiangning Analysis Instrument Company, China) as standard ASTM D-3801. The dimensions of samples tested were 125 mm × 13 mm × 3.2 mm. Five replicates were tested for each group.

Mechanical property tests

Mechanical properties were measured using a RGT-20A Universal Testing Machine (Shenzhen Reger Instrument Company, China). Tensile properties were carried out according to standard ASTM D-638 at a testing speed of 5 mm min^{-1}. Flexural properties were measured according to standard ASTM D-790 at a crosshead speed of 2 mm/min. The specimen dimension was 80 mm × 10 mm × 4 mm.

Cone calorimeter (CONE)

The cone calorimeter tests were carried out in accordance with the ASTM E1354 standard. Each specimen (100 × 100 × 3 mm^3) was wrapped in aluminum foil and exposed horizontally to an external heat flux of 50 kW m^{-2}. Three replicates were tested for each group.

Thermo-gravimetric (TG)

TG analysis was measured using a Pyris 1 Thermal Analyzer (PerkinElmer Company, America). Samples were measured under nitrogen or air at a heating rate of

Table 1 The formula of PP/WF composites

Samples	PP/%	WF/%	MA-g-PP/%	Antioxidant 1010/%	AP/%	MCA/%	Ratio (AP:MCA)
1	36.0	54.0	9.0	1.0	0	0	–
2	28.0	42.0	9.0	1.0	20.0	0	–
3	28.0	42.0	9.0	1.0	0	20.0	–
4	28.0	42.0	9.0	1.0	17.5	2.5	7:1
5	28.0	42.0	9.0	1.0	16.7	3.3	5:1
6	28.0	42.0	9.0	1.0	15.0	5.0	3:1
7	28.0	42.0	9.0	1.0	10.0	10.0	1:1
8	28.0	42.0	9.0	1.0	5.0	15.0	1:3
9	28.0	42.0	9.0	1.0	3.3	16.7	1:5
10	28.0	42.0	9.0	1.0	2.5	17.5	1:7

10 °C min^{-1} with a mass of 3–5 mg from 30 to 600 °C. Three replicates of each group were tested.

Fourier transform infrared spectrometry (FTIR)

The residues of PP/WF composites after LOI test were tested by a Nicolet 6700 spectrophotometer (Nicolette, USA). Each spectrum was collected with 4 cm^{-1} resolution in the range of 4000–500 cm^{-1}.

Scanning electron microscopy (SEM)

The morphologies of char residue were observed using a Quanta 200 Scanning Electron Microscopy (FEI Company, England). The thickness of specimens was about 2–3 mm, fixed on the sample stage and coated with a conductive layer of gold at the acceleration voltage of 5 kV.

Energy-dispersive X-ray spectroscopy (EDS)

The element content of surface residue was examined by INCA-type EDS instrument (the British Oxford Instrument Company). Specimens used to test were coated with a conductive layer of gold.

Results and discussion

LOI and UL-94 vertical tests

In order to investigate the flame retardance of the PP/WF composites, the LOI tests and UL-94 vertical tests were carried out at the room temperature. The results of LOI values and UL-94 rating for the samples are shown in Table 2. According to results, the sample 1 was highly flammable with low LOI value of only 23.8% and serious flaming dripping and failed in UL-94 test. The LOI values of sample 2 and sample 3 were increased to 27.7 and 27.2%, respectively, but the UL-94 tests were all failed, which indicated that the flame retardance of PP/WF composite was improved less obviously when AP and MCA were added solely. Nevertheless, the flame retardance of PP/WF composite was enhanced with the synchronous addition of AP and MCA, especially when the mass ratio of AP and MCA was 5:1. Sample 5 with AP/MCA (5:1) had the highest LOI value (29.5%) and passed V-0 rating with no flaming dripping. The results for the experiment demonstrated that the optimum mass ratio of AP and MCA was 5:1, and the minimum addition was 20%.

Table 2 The combustion results of PP/WF composites

Samples	UL-94	LOI/%	Flaming dripping
1	–	23.8	Yes
2	–	27.7	No
3	–	27.2	No
4	V-2	28.3	No
5	V-0	29.5	No
6	V-0	29.2	No
7	V-1	28.5	No
8	–	27.6	No
9	–	27.4	No
10	–	27.3	Yes

The morphologies of the char layers collected after LOI test were observed with both the front and side of samples. Figure 1 shows the digital photographs of the residue of PP/WF composites after LOI test. There was low-intensity and shapeless char residue remained for sample 1. Sample 2 presented an irregular intumescent char residue that was easy to collapse. There was nearly extremely thin char residue structure formed for sample 3 according to that the thickness of the sample was hardly changed before and after burning. However, sample 5 demonstrated an intumescent char residue which gave rise to high flame retardancy.

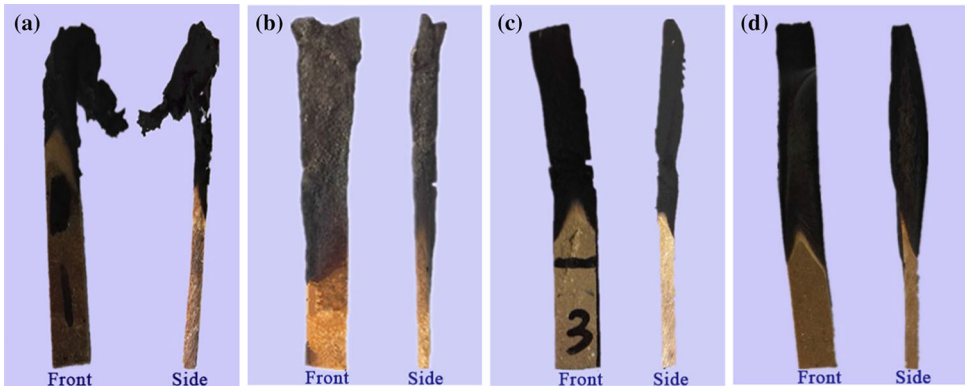

Fig. 1 Digital photographs of the residue of PP/WF composites after LOI test. **a** Sample 1, **b** sample 2, **c** sample 3, **d** sample 5

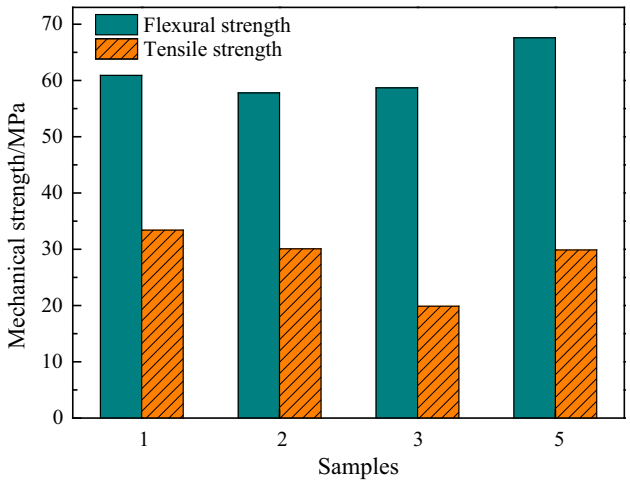

Fig. 2 The mechanical properties of PP/WF composites

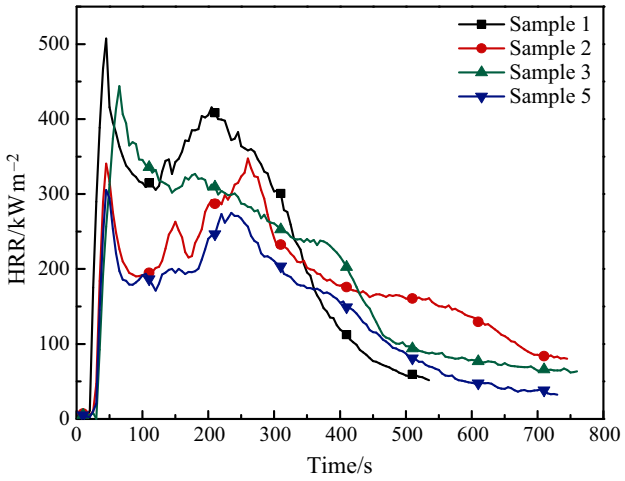

Fig. 3 Heat release rate (HRR) curves of PP/WF composites

Mechanical properties

The mechanical properties of materials are a main parameter for evaluating materials. Figure 2 indicates that the mechanical properties of PP/WF composites were significantly changed after mixing with flame retardant. Compared with sample 1, the tensile strengths of PP/WF composites were all reduced with the incorporating of flame retardant, while that of sample 5 was reduced less by 3.5 MPa. However, it was observed that the flexural strength of sample 5 was increased by about 11.0% in comparison with sample 1. It was possible that the addition of AHP as inorganic salt and MCA as activated salt increased the polarity of WF, which destroyed cohesion between PP and WF and dropped interfacial compatibility, and then reduced tensile strength. Nevertheless, due to the excellent lubricity of AHP and MCA and the outstanding compatibility between PP and MCA, the flexural strength of the composite was improved.

Table 3 Cone calorimeter test data

Samples	IT/s	PHRR/kW m^{-2}	THR/MJ m^{-2}
1	23	507.2	128.3
2	32	347.5	108.3
3	37	443.9	122.0
5	34	304.1	97.9

Table 4 TGA and DTG data of PP/WF composites

Samples	$T_{5\%}$/°C	T_1/°C	T_2/°C	T_3/°C	Char residue/% 600 °C
1	283.1	–	358.8	494.5	18.8
2	294.8	321.5	357.2	499.1	34.3
3	293.6	348.2	388.7	501.5	14.7
5	295.9	318.2	340.6	510.4	32.8

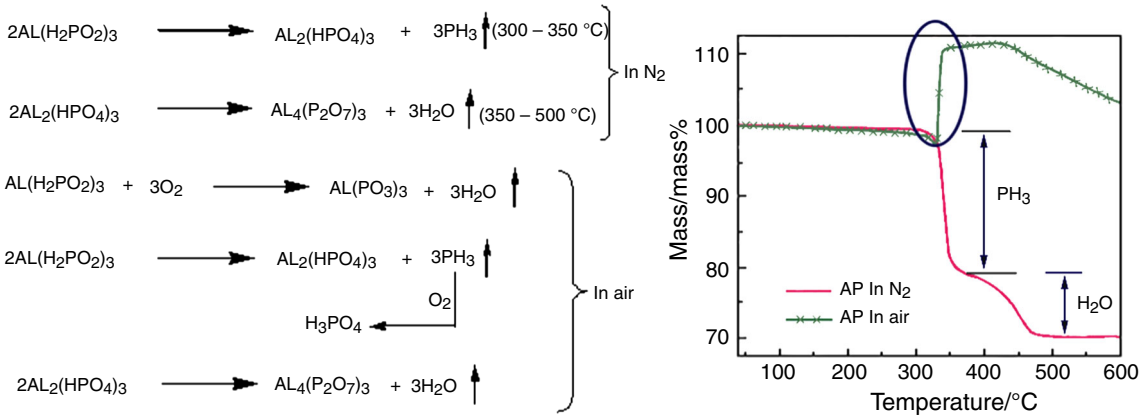

Fig. 4 The thermal degradation mechanisms and thermo-gravimetric analysis of AP

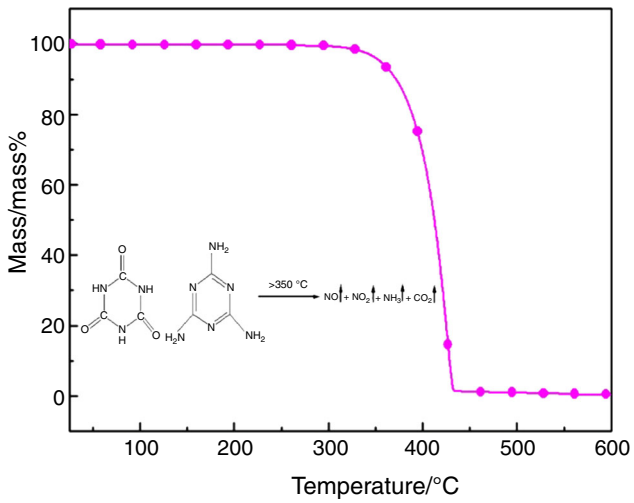

Fig. 5 The thermal degradation mechanisms and thermo-gravimetric analysis of MCA

Cone calorimetric analysis

The cone calorimetry is one of the most effective methods to evaluate the flame properties of materials. In order to probe into the effect of AP/MCA on the flame retardance of PP/WF composite, cone calorimeter test was carried out under air. The HRR tested by cone calorimeter is a crucial parameter as it presents the intensity of a fire. Figure 3 and Table 3 demonstrate the outcomes of cone calorimeter of samples 1, 2, 3 and 5 at heat flux of 50 kW m^{-2}.

As shown in Fig. 2, sample 1 burned fast after ignition and had the highest heat release rate (HRR) curve with a heat release rate peak (PHRR) of 507.2 kW m^{-2}, whereas the PHRR value of samples 2, 3 and 5 reduced to 347.5, 443.9 and 304.1 kW m^{-2} , respectively with the addition of AP and MCA. It was noted that the PHRR of sample 5 decreased more quickly than others, revealing the synergistic effect of AP and MCA. According to Table 4, it was very clear that sample 5 showed the longer ignition time (IT) than sample 1 and had the lowest THR value. All the

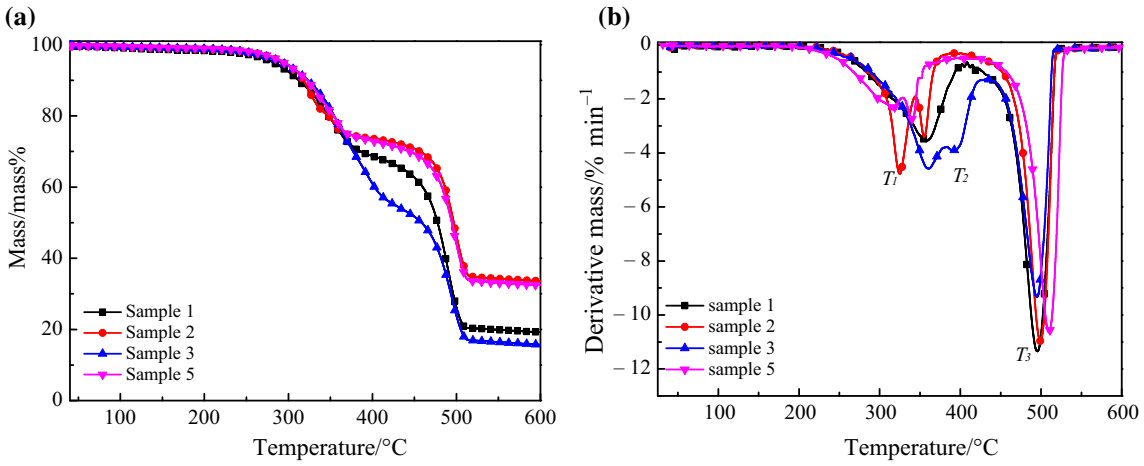

Fig. 6 TGA (**a**) and DTG (**b**) curves of PP/WF composites

cone calorimetric data demonstrated that AP/MCA was an effective flame retardant for PP/WF composite.

TG analysis

The thermal degradation of AP and MCA

Aluminum phosphinate (AP) was analyzed by thermo-gravimetry in nitrogen and air atmosphere. The thermal degradation mechanisms and thermo-gravimetric analysis of AP [23–25] are shown in Fig. 4. In nitrogen atmosphere, the thermal decomposition of AP was characterized by two steps. The decomposition of AP mainly produced PH_3 and H_2O at the first and second steps, respectively, leaving the residue of $Al_4(P_2O_7)_3$. However, the thermal degradation behavior of AP in air atmosphere was different from that in nitrogen atmosphere. There was a sharp mass increment of residue for AP in the air, which may result from the oxidation of AP.

The thermal decomposition mechanisms and thermo-gravimetric analysis of MCA under nitrogen condition are shown in Fig. 5. The thermal degradation of MCA began from 350 °C. And only a few residues (close to zero) remained at 600 °C. It is revealed that MCA mainly released gas-phase products such as CO_2, NH_3, NO and NO_2 during thermal decomposition [22, 26].

The thermal degradation of PP/WF composites

The thermal degradation of PP/WF composites was studied by TG under nitrogen condition. The TG and DTG curves of PP/WF composites are shown in Fig. 6a, b. The temperature at 5% mass loss ($T_{5\%}$), the first peak temperature (T_1), the second peak temperature (T_2), the third peak temperature (T_3) and the char residue at 600 °C are listed in Table 4. The thermal degradation processes of sample 1 underwent two steps, and that of samples 2, 3 and 5 went through three steps. For sample 5, the thermal degradation of the first step was attributed to AP, and the second step was assigned to the degradation of MCA and WF. Subsequently, PP occurred thermal degradation in the third step. With AP and MCA incorporated into the composite, $T_{5\%}$ of sample 5 was increased by 12.8 °C and T_2 of sample 5 was reduced by 18.2 °C compared with sample 1. It meant the thermal decomposition of WF was advanced and the stability of the composite was enhanced in lower temperature. The decomposition products of AP accelerated the thermal decomposition of WF by esterification reaction with WF. T_3 of sample 5 was increased to 510.4 °C, which meant the high-temperature stability of the composite was enhanced due to the protection of intumescent layer.

By comparison, the actual char residue of sample 1 was 18.8% at 600 °C, whereas that of sample 3 was reduced by 21.8% compared with sample 1 unexpectedly. The probable reason was that MCA was mainly resolved into gases. The char residue of sample 5 was 32.8% higher than that of sample 1, which exceeded the calculation result of 30.8% that acquired from the count based on the char residue obtained from experiment and mass ratio of samples 2 and 3 likewise.

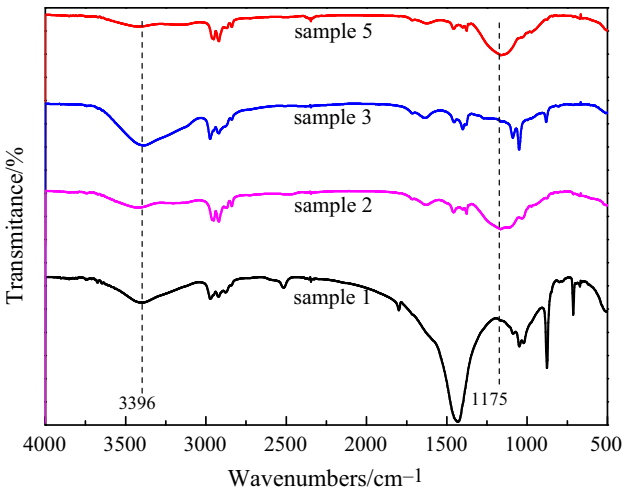

Fig. 7 FTIR spectra of the char layers for different PP/WF composites

FTIR analysis

The spectra of char layers for samples 1, 2, 3 and 5 after LOI test are shown in Fig. 7. The absorption occurring at 3396 cm^{-1} was attributed to the bending of O–H and was gradually weakened for sample 5. The absorption band of 1175 cm^{-1} represented for P–O–C group was observed in samples 2 and 5, while the spectra of samples 1 and 3 showed almost no absorption, and the peak of sample 5 was stronger than that of sample 2. It was revealed that the products of AP such as $Al_2(HPO_4)_3$ and H_3PO_4 catalyzing the formation of P–O–C cross-linked char layers by esterification reaction with O–H group of WF. Except that the peak of ring stretching (1300–1600 cm^{-1}) of aromatic heterocycle was broke up into multiple peaks compared with the spectra of sample 1, the spectra of sample 3 had the same behavior as that of sample 1. It was indicated that MCA mainly produced gases during the thermal decomposition processes of composite.

Morphology of the residual char

The microstructure of char layers of PP/WF composites was viewed via SEM, as shown in Fig. 8. The surface char residue morphology of sample 1 is shown in Fig. 8a, and it demonstrated a mussy and loose char layer with some

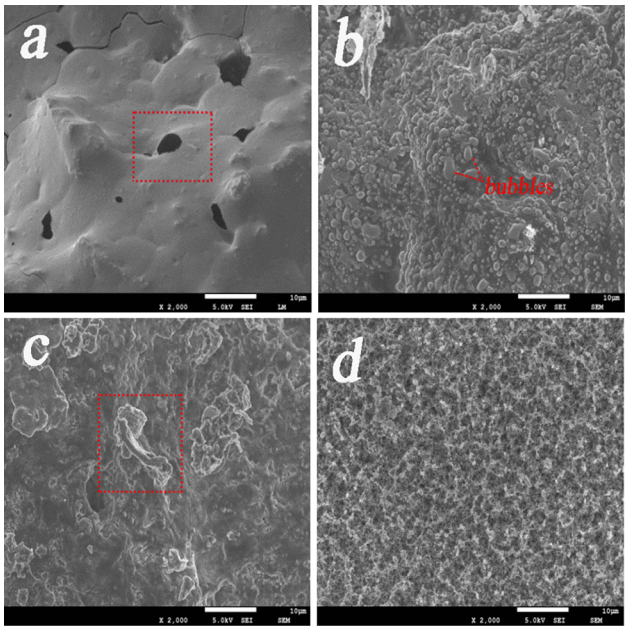

Fig. 8 Residue morphologies of PP/WF composites. **a** Sample 1, **b** sample 2, **c** sample 3, **d** sample 5

macropores and cracks diffusing at the surface. In accordance with Fig. 8b, sample 2 shows an irregular char layer together with bubbles dispersing at the surface, caused by the degradation products of AP such as PH_3 and H_2O [25]. The surface char residue morphology of sample 3 was similar to fluid with no char residue structure observed, thereby indicating again that the addition of MCA had little

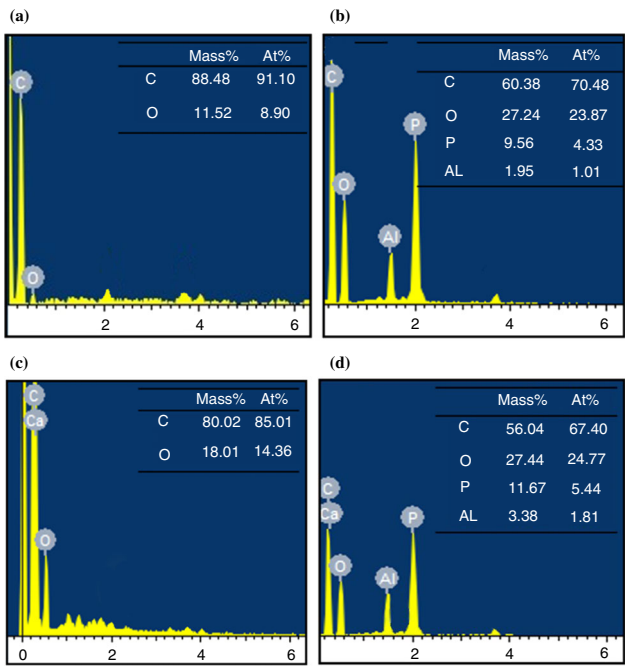

Fig. 9 EDS results of residues of PP/WF composites after LOI test. **a** Sample 1, **b** sample 2, **c** sample 3, **d** sample 5

effect on forming char residue. Figure 8d shows the char residue morphology of sample 5, and uniform intumescent char residue structure at the surface was exhibited. That many diminutive and uniform particles formed three-dimensional interpenetrating networks [24] and many tiny pores dispersed in the char residue uniformly were observed. These pores were generated by the procreant gases of MCA and AP. These released gases accelerated the char to expand and diluted oxygen and flammable gases during combustion process, achieving the aim of condensed-phase and gas-phase flame retardancy. That more uniform char residue structure had more effect on hindering the spreading of oxygen and heat into the interior.

EDS analysis

The elemental contents of the surface char layers for samples 1, 2, 3 and 5 after LOI test were detected by EDS test, as shown in Fig. 9. The relative C content of the surface char residue for samples 2, 3 and 5 was all reduced compared with sample 1, while that of sample 5 suffered the biggest drops with 36.7%. It was because of the incomplete degradation of the composite. The mass percent of O for sample 5 was increased to 27.44% higher than other three samples, and the relative contents of P and Al were increased from 9.56 and 1.95% to 11.67 and 3.38%, respectively, in comparison with sample 2. It was indicated that MCA can stimulate the thermal decomposition of AP to form more products based on PO_4^{3-} and Al such as H_3PO_4 and $Al_2(HPO_4)_3$. It should be also noticed that there was no N element observed in the surface residue for sample 3, suggesting that the N elements of MCA were released by the way of gases like NH_3, NO and NO_2.

Thermal property reinforcing mechanism

The thermal property reinforcing mechanism based on the results of TGA, FTIR and EDS tests and some interrelated literature [22–27] is exhibited in Fig. 10. At the temperature of 300–350 °C, AP decomposed prior to WF to release $Al_2(HPO_4)_3$ and PH_3 which was oxidized to H_3PO_4 to react with O–H of WF, forming a P–O–C cross-linked layer. Meanwhile, MCA decomposed to generate gases such as NO_2, NH_3, NO and CO_2, which diluted flammable gases and accelerated the char residue to inflate. Above 350 °C, PP started to decompose and more thermally stable char layer came into being. The stable char layer acted as a physical barrier to prevent the fire from transferring into inner materials and resist the evolution of flammable gases. The relieving inert gases acted as a gas shield on the surface of material and reduced the combustion reaction of flammable gases. It summarized that condensed-phase and

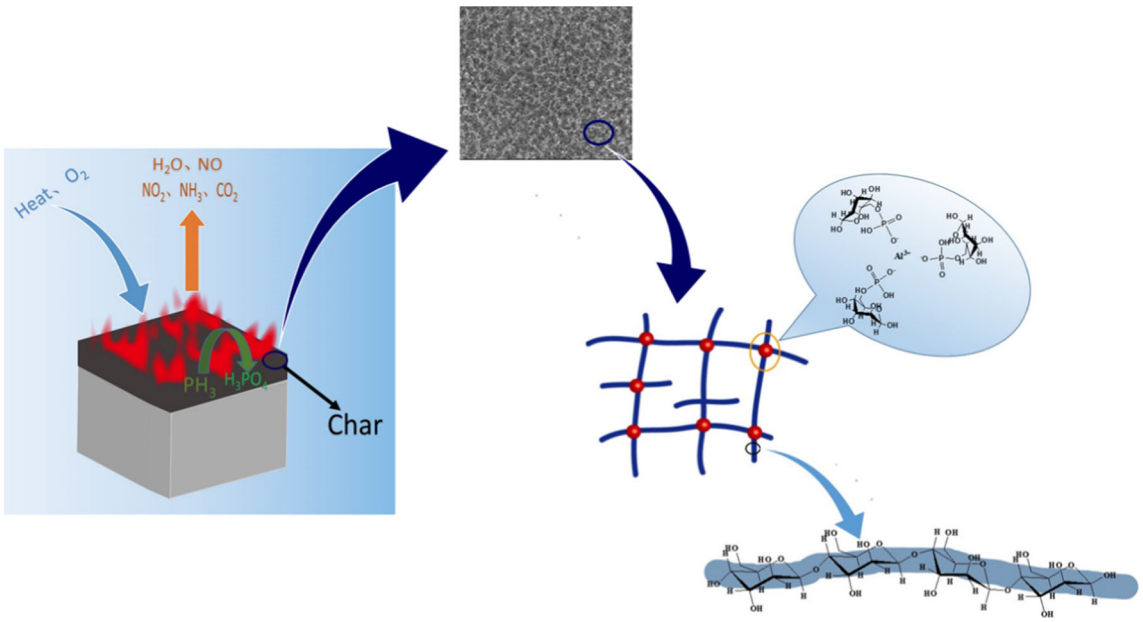

Fig. 10 Possible flame-retardant mechanism of AP/MCA for PP/WF composites

gas-phase flame-retardant mechanism acted together to enhance the flame retardancy of the PP/WF composite.

Conclusions

The PP/WF composite possessed the highest flammability at the optimal ratio of AP/MCA (5:1) with 20% loading. It was revealed that there was a combination of gas-phase and condensed-phase flame retardance during the combustion, and the thick P–O–C cross-linked char layer was formed so as to hinder the transfer of heat and flammable gases into the interior. Besides, the gases were generated during combustion and contributed to restricting the fire in gas phase. Thus, the combination of AP and MCA had been certified to be a forward-looking flame-retardant system for PP/WF composite.

Acknowledgements This work was financially supported by the National Natural Science Foundation of China (31570572 and 31670516) and Heilongjiang Key Project Technologies R&D Programme (GA15A101).

References

1. Klyosov AA. Wood-plastic composites. Hoboken: Wiley; 2007.
2. Zhang QF, Cai HZ, Yang KY, Yi WM. Effect of biochar on mechanical and flame retardant properties of wood-plastic composites. Results Phys. 2017;7:2391–5.
3. Hazarika A, Maji TK. Thermal decomposition kinetics, flammability, and mechanical property study of wood polymer nanocomposite. J Therm Anal Calorim. 2014;115:1679–91.
4. Jacob A. WPC industry focuses on performance and cost. Reinf Plast. 2006;50:32–3.
5. Sun LC, Wu QL, Xie YJ, Song KL, Lee SY, Wang QW. Thermal decomposition of fire-retarded wood flour/polypropylene composites. J Therm Anal Calorim. 2016;123:309–18.
6. Enamul Hoque M, Aminudin MAM, Jawaid M, Islam MS, Saba N, Paridah MT. Physical, mechanical, and biodegradable properties of meranti wood polymer composites. Mater Des. 2014;64:743–9.
7. Wu QL, Chi K, Wu YQ, Lee SY. Mechanical, thermal expansion, and flammability properties of co-extruded wood polymer composites with basalt fiber reinforced shells. Mater Des. 2014;60:334–42.
8. Annette N, Ina S, Matthias N. Material resistance of flame retarded wood-plastic composites against fire and fungal decay. Int Biodeterior Biodegrad. 2012;75:28–35.
9. Ayrilmis N, Akbulut T, Dundar T, White RH, Mengeloglu F, Buyuksari U, Candan Z, Avci E. Effect of boron and phosphate compounds on physical, mechanical, and fire properties of wood-polypropylene composites. Constr Build Mater. 2012;33:63–9.
10. Fang YQ, Wang QW, Guo CG, Song YM, Cooper PA. Effect of zinc borate and wood flour on thermal degradation and fire retardancy of polyvinyl chloride (PVC) composites. J Anal Appl Pyrol. 2013;100:230–6.
11. Wang DY, Leuteritz A, Kutlu B, der Landwehr MA, Jehnichen D, Wagenknecht U, Heinrich G. Preparation and investigation of the combustion behavior of polypropylene/organomodified MgAl-LDH micro-nanocomposite. J Alloys Compd. 2011;509:3497–501.
12. Bai G, Guo CG, Li LP. Synergistic effect of intumescent flame retardant and expandable graphite on mechanical and flame-retardant properties of wood flour-polypropylene composites. Constr Build Mater. 2014;50:148–53.
13. Michael R, Clemens S, Uwe M, Harald S. Determination of reaction mechanisms and evaluation of flame retardants in wood-melamine resin-composites. J Anal Appl Pyrol. 2007;79:306–12.
14. Seefeldt H, Braun U, Wagner MH. Residue stabilization in the fire retardancy of wood-plastic composites: combination of

ammonium polyphosphate, expandable graphite, and red phosphorus. Macromol Chem Phys. 2012;213:2370–7.
15. Covaci A, Harrad S, Abdallah MAE, Ali N, Law RJ, Herzke D, de Wit CA. Novel brominated flame retardants: a review of their analysis, environmental fate and behavior. Environ Int. 2011;37:532–56.
16. Nie SB, Peng C, Yuan SJ, Zhang MX. Thermal and flame retardant properties of novel intumescent flame retardant polypropylene composites. J Therm Anal Calorim. 2013;113:865–71.
17. Guan YH, Huang JQ, Yang JC, Shao ZB, Wang YZ. An effective way to flame-retard biocomposite with ethanolamine modified ammonium polyphosphate and its flame retardant mechanisms. Ind Eng Chem Res. 2015;54:3524–31.
18. Jiang D, Pan MZ, Cai X, Zhao YT. Flame retardancy of rice straw-polyethylene composites affected by in situ polymerization of ammonium polyphosphate/silica. Compos Part A. 2018;109:1–9.
19. Ge H, Tang G, Hu WZ, Wang BB, Pan Y, Song L, Hu Y. Aluminum hypophosphite microencapsulated to improve its safety and application to flame retardant polyamide 6. J Hazard Mater. 2015;294:186–94.
20. Zhao B, Chen L, Long JW, Chen HB, Wang YZ. Aluminum hypophosphite versus alkyl-substituted phosphinate in polyamide 6: flame retardance, thermal degradation, and pyrolysis behavior. Ind Eng Chem Res. 2013;52:2875–86.
21. Lu XS, Qiao XY, Yang T, Sun K, Chen XD. Preparation and properties of environmental friendly nonhalogen flame retardant melamine cyanurate/nylon 66 composites. J Appl Polym Sci. 2011;122:1688–97.
22. Liu Y, Wang Q. The investigation on the flame retardancy mechanism of nitrogen flame retardant melamine cyanurate in polyamide 6. J Polym Res. 2009;16:583–9.
23. Yan YW, Huang JQ, Guan YH, Shang K, Jian RK, Wang YZ. Flame retardance and thermal degradation mechanism of polystyrene modified with aluminum hypophosphite. Polym Degrad Stab. 2014;99:35–42.
24. Wu NJ, Li XT. Flame retardancy and synergistic flame retardant mechanisms of acrylonitrile-butadiene-styrene composites based on aluminum hypophosphite. Polym Degrad Stab. 2014;105:265–76.
25. Yuan BH, Bao CL, Guo YQ, Song L, Liew KM, Hu Y. Preparation and characterization of flame-retardant aluminum hypophosphite/poly(vinyl alcohol) composite. Ind Eng Chem Res. 2012;51:14065–75.
26. Ceyda I, Jale H. Investigation of thermal degradation characteristics of polyamide-6 containing melamine or melamine cyanurate via direct pyrolysis mass spectrometry. J Anal Appl Pyrol. 2012;98:221–30.
27. Jiao YH, Wang XL, Wang YZ, Wang DY, Zhai YL, Lin JS. Thermal degradation and combustion behaviors of flame-retardant polypropylene/thermoplastic polyurethane blends. J Macromol Sci B. 2009;48:887–909.